Supplementary Material: Hole Doped Nonvolatile and Electrically Controllable Magnetism in van der Waals Ferroelectric Heterostructures

Xinxin Jiang(姜新新)[1], Zhikuan Wang(王智宽)[1], Chong Li(李冲)[2], Xuelian Sun(孙雪莲)[1], Lei Yang(杨磊)[1], Dongmei Li(李冬梅)[1,*], Bin Cui(崔彬)[1,*], and Desheng Liu(刘德胜)[1,*]

[1]School of Physics, National Demonstration Center for Experimental Physics Education, Shandong University, Jinan 250100, China.
[2]School of Physics and Microelectronics, Zhengzhou University, Zhengzhou 450001, China

*Corresponding authors. Email: li_dm@sdu.edu.cn; cuibin@sdu.edu.cn; and liuds@sdu.edu.cn

Crystal structures

The calculated lattice constants are 4.06 and 4.07 Å for InSe and In_2Se_3, respectively. Their lattice constants are comparable with almost no lattice mismatch. Next, we have considered three possible stacking configurations, as shown in Figure S1, labeled as In-In, Se-Se, and Se-In stacking patterns. We have imposed a commensurability condition between the InSe and In_2Se_3 monolayers, where a 1×1 lateral periodicity is employed. From Table S1, we found that these electronic characteristics exhibit similar behavior. Moreover, all the calculated binding energies are negative, indicating that all the considered stacking patterns are energetically stable. In particular, we observe that there is little difference in the binding energy between the different stacking patterns of each heterostructure. So, for convenience, we only study the In-In stacking as an example in the following calculations since it has the lowest binding energy.

I. Stability calculations

To assess the stability of the heterostructures, we calculate the binding energy (E_b) using the formula:

$$E_b = \left(E_{InSe/In_2Se_3} - E_{InSe} - E_{In_2Se_3} \right) / N$$

where E_{InSe/In_2Se_3}, E_{InSe}, and $E_{In_2Se_3}$ are the total energies of vdWH, InSe, and In_2Se_3 monolayers, respectively, and N is the number of atoms. From Table S1 can be seen that the calculated binding energies of vdWHs are negative, suggesting that the attractive interfacial interaction between InSe and In_2Se_3 layers is energetically favorable.

Moreover, the phonon dispersions are calculated with the density functional perturbation theory by using the PHONOPY code. The interatomic forces are computed using the VASP code. The tolerance for the energy convergence used for the phonon calculations was 10^{-8} eV·Å^{-1}. 6 × 6 × 1 supercell with 3 × 3 × 1 *k*-mesh is used to ensure the convergence. As shown in Figure. S2, no appreciable imaginary vibrational frequency modes are observed in the entire Brillouin zone, proving that the heterostructure is kinetically stable.

II. Monte Carlo simulation

To predict the Curie temperature (Tc) of these heterostructures, Monte Carlo (MC) simulations were performed based on the Heisenberg model. Without an external field, the Hamiltonian of the Heisenberg model is described by:

$$H = -\sum_{\langle i,j \rangle} J_{ij} \hat{S}_i \hat{S}_j - D \sum_i (\hat{S}_i^z)^2$$

where J_{ij} is the exchange coupling constant between i and j sites, $\hat{S}_i$ and $\hat{S}_j$ are spin operators. D represent the magnetic anisotropy energy, which is calculated from the energy difference of magnetization along z and x/y axis, with a value of 0.2 meV. the energies of the FM and AFM states are:

$$E_{FM} = E_0 - 6JS^2$$

$$E_{AFM} = E_0 + 2JS^2$$

here, E_0 is the system energy without considering the spin degree of freedom. The

value of exchange integral J_{ij} is about 24.91 meV, obtained by calculating energies of FM and AFM states. In the MC simulations, we used a 200×200 supercell to reduce the periodic constraints. At each temperature, 5×10^5 loops are taken to achieve an average magnetic moment value. The variation of the magnetic moment per unitcell with respect to temperature is plotted in Figure. S4 (c). We see that the magnetic moment per unitcell starts to drop gradually from 0.5 μB and The T_C of 84 K was read from the peak position of the specific heat defined as $C_V = (\langle E^2 \rangle - \langle E \rangle^2) / (k_B T^2)$.

According to the Stoner model, the ferromagnetic state is stabilized by the condition:

$$\Delta = Im,$$

where Δ is the exchange splitting of the spin-up and spin-down bands (VB in our case), I is the Stoner parameter, and m is the magnetization density ($m = n_\uparrow - n_\downarrow$), $n_\uparrow$ ($n_\downarrow$) is the total number of electrons in spin up (down) channel. From the total DOS under each doping condition, we can get Δ and m. For doping concentrations of 9.75×10^{14}/cm^2, Δ is approximately 0.375 eV of VB, and m is 0.88, and, thus, I is 0.426 eV. According to Stoner criterion, the spin splitting will occur when

$$D(E_F) \times I > 1,$$

where $D(E_F)$ is the total density of state (DOS) at the Fermi level.

The valance bands have local maxima near the E_F. And they cause the large density of states near the E_F. Therefore, with a small change in doping concentration, the DOS at the Fermi level will be large. When the doping concentration is 9.75×10^{14}/cm^2, the resulting DOS (5.261 states/eV) is sufficient to cause spin splitting.

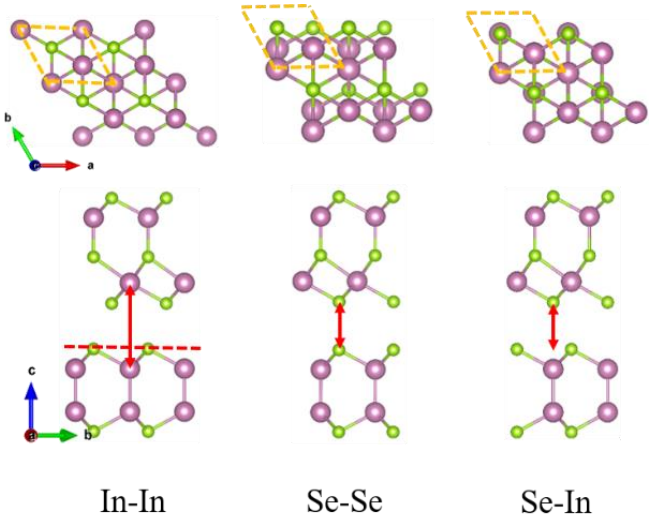

Fig. S1. Three stacking patterns of $InSe/In_2Se_3$ vdWHs.

Table S1 Calculated lattice constant (a), bandgap (E_g) obtained by the PBE, binding energy (E_b), and interlayer distance (d).

	a (Å)	E_g (eV)	E_b (meV per atom)	d (Å)
InSe	4.06	1.53		
In_2Se_3	4.07	0.81		
In–In (P↑)	4.07	0.45	–30.04	2.95
In–In (P↓)	4.07	0.48	–28.27	3.00
Se–Se (P↑)	4.08	0.49	–27.27	3.13
Se–Se (P↓)	4.07	0.54	–17.92	3.77
Se–In (P↑)	4.07	0.46	–29.38	3.04
Se–In (P↓)	4.07	0.47	–28.26	3.06

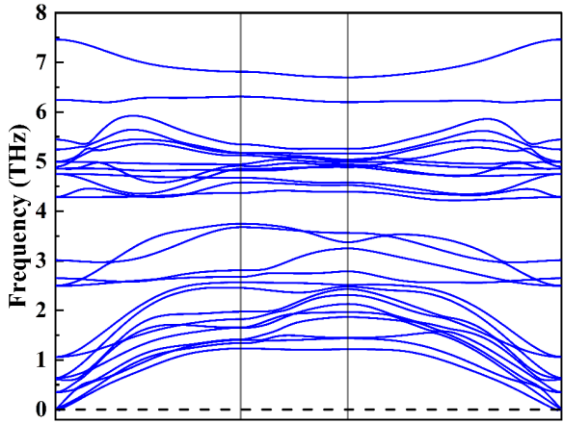

Fig. S2. Phonon band dispersion for $InSe/In_2Se_3$ vdWH.

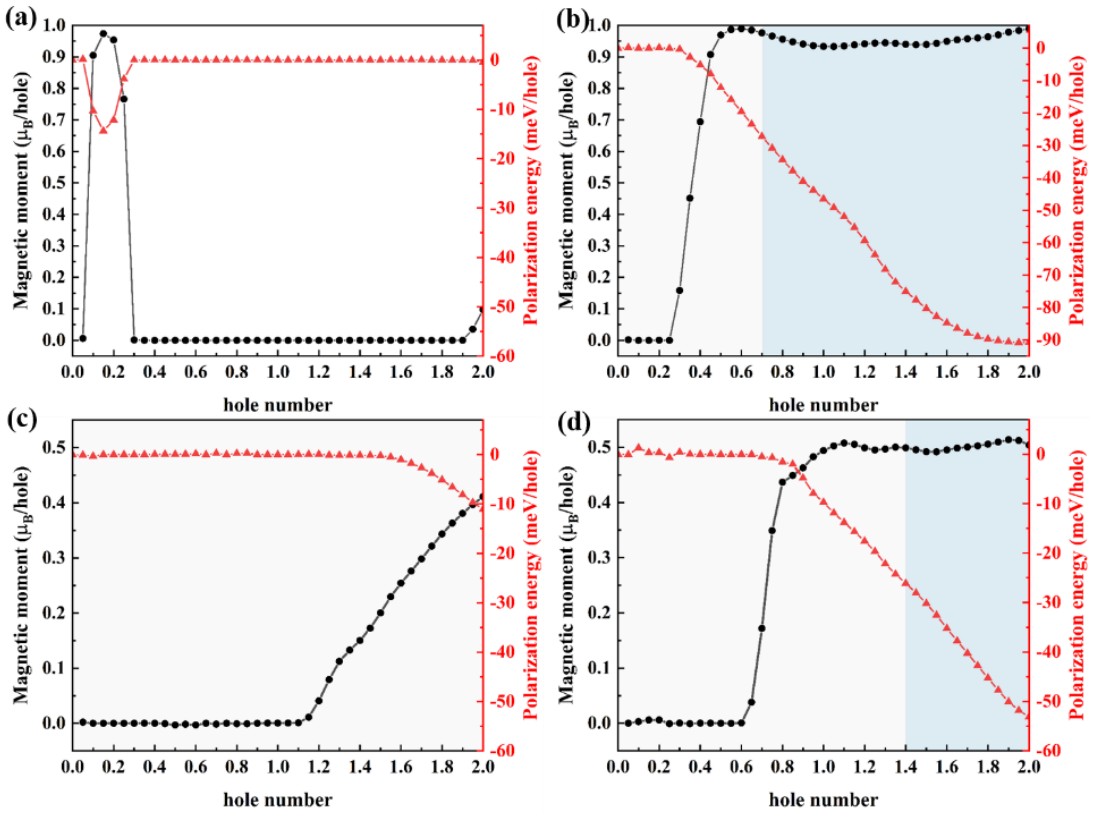

Fig. S3 Doping level dependence of the magnetic moment (black curve) and magnetization energy (red curve) for (a) InSe, (b) In_2Se_3, (c) InSe/In_2Se_3 (P↑), and (d) InSe/In_2Se_3 (P↓), respectively, where μ_B is the Bohr magneton. The light blue regions indicate large spin polarization energies.

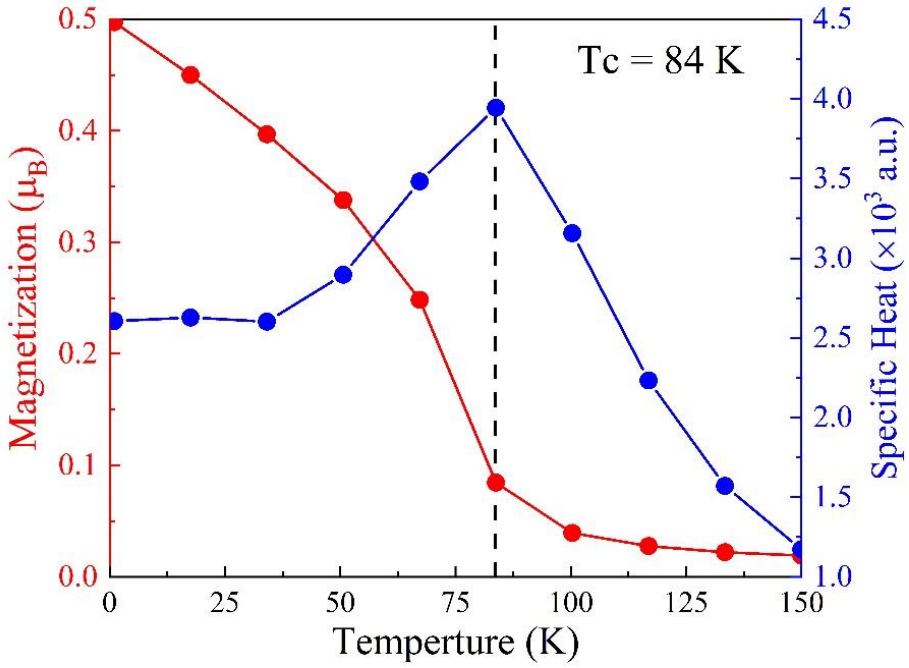

Fig. S4 Temperature-dependent average magnetic moment per unitcell obtained by Monte Carlo simulations based on the Heisenberg model.

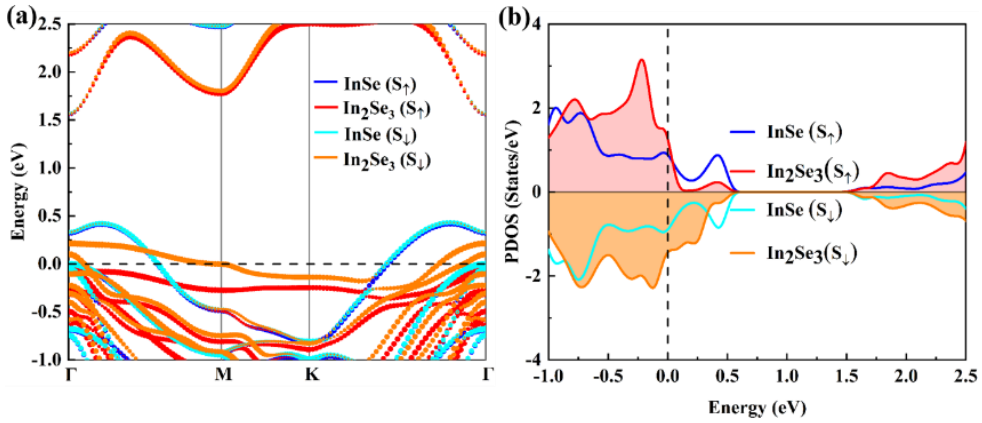

Fig. S5 (a) Spin-polarized band structure and (b) spin-polarized PDOS of InSe/In_2Se_3 (P↑) vdWH under a hole density of $9.75\times10^{14}/cm^2$. Blue (red) and cyan (orange) lines represent the contributions of the InSe (In_2Se_3) layer with the spin-up and spin-down bands, respectively. The E_F is set at zero and marked with the black dashed line.

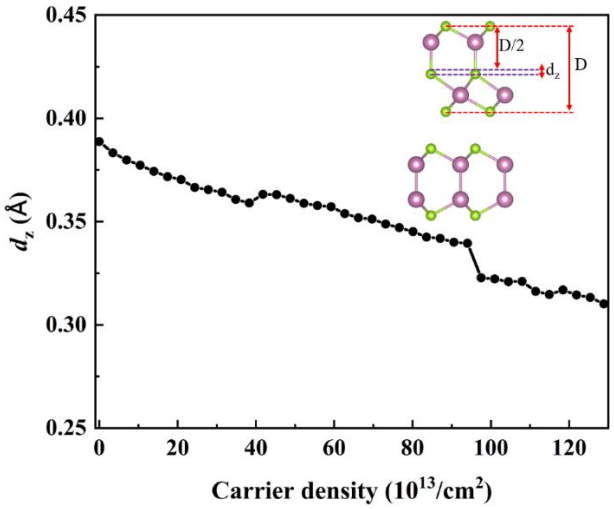

Fig. S6 Polar atomic displacement (d_z) as a function carrier density for the InSe/In_2Se_3 vdWH (P↓). The insets illustrate the definitions of d_z in InSe/In_2Se_3 vdWH (P↓).

Table S2. Total energies 2×2 supercell of InSe/In_2Se_3 vdWH under NM, FM and AFM.

	Total energy (eV)
NM	-135.789929
AFM	-135.788973
FM	-135.789727